Analytical Modeling of Flat Face Flanges With Metal-to-Metal Contact Beyond the Bolt Circle

Hichem Galai
e-mail: hichem.galai.1@ens.etsmtl.ca

Abdel-Hakim Bouzid
Professor
e-mail: hakim.bouzid@etsmtl.ca

Department of Mechanical Engineering,
Ecole de Technologie Superieure,
1100 Rue Notre-Dame Ouest,
Montreal, QC, H3C 1K3, Canada

Design rules for flat face flanges with metal-to-metal contact beyond the bolt circle are covered by Appendix Y of the American Society of Mechanical Engineers Code. These design rules are based on Schneider's work (1968, "Flat Faces Flanges With Metal-to-Metal Contact Beyond the Bolt Circle," ASME J. Eng. Power, ***90****(1), pp. 82–88). The prediction of tightness of these bolted joints relies very much on the level of precision of the self-sealing gasket compression during operation. The evaluation of this compression requires a rigorous flexibility analysis of the joint including bolt-flange elastic interaction. This paper analyses flange separation and the bolt load change in flat face bolted joints. It proposes two different analytical approaches capable of predicting flange rotation and bolt load change during operation. The first method is based on the beam theory applied to a continuous flange sector. This approach is an improvement of the discrete beam theory used in the Schneider model. The second method is based on the circular plate theory and is developed for the purpose of a more accurate assessment of the load changes. As in the Taylor Forge method, this approach is, in general, better suited than the beam theory for flat face flanges, in particular when the flange width is small. The proposed models are compared with the discrete beam theory and validated using numerical finite element analysis on different flange sizes.*
[DOI: 10.1115/1.4001655]

1 Introduction

Before the advent of digital methods, a multitude of approaches, theories, and experimental studies had been conducted in order to analyze the behavior of bolted flange joints with metal-to-metal contact beyond the bolt circle. In 1967, Webjörn [1] laid out the first basics of a design method of this type of assembly. Later, Schneider [2] used a beam theory model to solve flanges with metal-to-metal contact. His method was quickly adopted by the American Society of Mechanical Engineers (ASME) Code and forms the basis of Appendix Y [3]. Pindera and Sze [4] focused on experimental methods to determine the influence of the bolts with washers on the flange metal-to-metal contact. The authors have identified the seat preload and rigidity of the bolts as design parameters. They noted that increased values of these parameters reduces the load on the bolts in the operating conditions and increases the contact pressure between the two flanges. Webjörn and Schneider [5] applied their theoretical and experimental findings to another type of metal-to-metal contact flanges known as compact flanges. No sign of separation was observed below a bolt preload of 80% of the elastic limit. The authors noted 6% bolt load change at higher pressure, which lead them to conclude that cyclic pressure below a certain limit does not cause fatigue of the bolts or the deterioration of the joint.

Webjörn [6,7] compared the different metal-to-metal contact flanges with and without the application of external loads, such as the bending moments and misalignment shear loads, taking into account the effect of temperature and corrosion. He concludes that the tension on the bolts increases on average by 5% due to external efforts and offered some practical advice for the design of assemblies. Webjörn [8] stated that the ASME Code flange design is conservative because the elements of the assembly are designed separately. He recommended a comprehensive study that takes into account the interaction between all components. Lewis et al. [9] described a method for determining the initial gap between flat face flanges with initial wedge before applying pressure. They considered various configurations and wide flanges with positive and negative slopes. They observed that, in the case of the flange with a positive slope, the initial rate of leakage increases dramatically with the extension bolts. While in the case of the flange with a slightly negative slope, the leakage rate decreases with the initial expansion bolts. Lewis et al. concluded that the leak rate in a slightly negative slope case is less sensitive to the bolt hydrostatic end force and bolt stretch, whereas the leak rate in a slightly positive slope case is very sensitive to the bolt stretch. They added that the quality of the surface flanges plays a crucial role in the seal and has a greater influence than the distortion induced by the crushing of the joint. Fessler et al. [10] conducted a linear elastic finite element deflection study on flanges with wedges. The authors concluded that for flanges with a slightly positive slope, the leak paths are closed, if the bolts are tight enough, and therefore, the leak rate decreases considerably. Hyde et al. [11,12] continued the finite element work of Fessler and added experimental studies to determine the tension on the bolts and the loss of contact pressure between the flanges. They noted that the flanges with a small slope are tighter that those of flat and parallel faces. They mentioned that the effect of the axial load is the most dominant among the efforts applied. This dominance is intensified when the contact surface decreases. Most of the recent work on flanges with metal-to-metal flanges is dedicated toward the study of compact flanges. References [13–16] gave comparative and parametric studies on compact flanges.

A new approach that considers the flange as a plate with a central hole is presented. The one-dimensional aspect of the flange considered by Schneider is to be verified. In addition, referring to Schneider's work [2], the flange ring could be treated as an annular plate with either clamped ends or simply supported ends, depending on the remaining contact area. This paper compares three models—discontinuous beam model, continuous beam model, and plate model—against the more accurate FE analyses and discusses a few parameters of design importance.

Contributed by the Pressure Vessel and Piping Division of ASME for publication in the Journal of Pressure Vessel Technology. Manuscript received August 17, 2009; final manuscript received November 26, 2009; published online October 19, 2010. Assoc. Editor. William J. Koves.

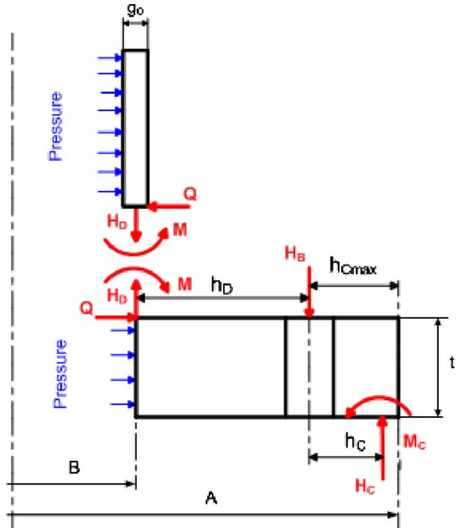

Fig. 1 Flange analytical model

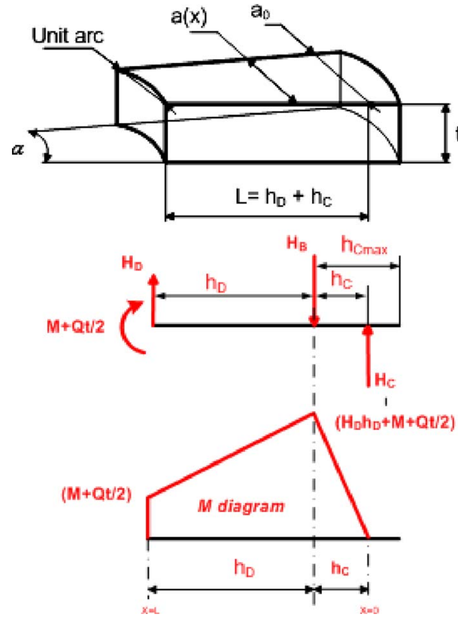

Fig. 2 Free body diagram of the continuous beam

2 Analytical Modeling

The complex structure of the bolted joint may be represented by the structural elements of a known behavior, the free body diagram of which can be drawn with forces and moments applied, as shown in Fig. 1. In the analysis, the gasket located near the bore is soft enough so as its reaction is small compared with the initial bolt load. Applying the force and moment equilibrium together with the continuity of displacement and rotation generates a system of equations that can be used to solve for the unknowns M, Q, H_B, H_C, and M_C.

First, applying the theory of beams on the elastic foundation [17] to determine the displacement and rotation of the cylinder at the junction with the flange subjected to internal pressure and discontinuity edge loads Q and M yields

$$u_s = \frac{6(1-\nu^2)}{Eg_0^3\beta^3}Q - \frac{6(1-\nu^2)}{Eg_0^3\beta^2}M + \frac{(2-\nu)B^2}{8Eg_0}P \tag{1}$$

$$\theta_s = \frac{12(1-\nu^2)}{Eg_0^3\beta^3}M - \frac{6(1-\nu^2)}{Eg_0^3\beta^2}Q \tag{2}$$

The radial flange displacement considered as a thick cylinder is given by

$$u_f = \frac{B\gamma P}{2E} - \frac{B\gamma Q}{2tE} + \frac{t}{2}\theta_f \tag{3}$$

Establishing compatibility between the cylinder and flange gives a system with two equations and three unknowns Q, M, and flange rotation θ_f. The system is statically indeterminate and requires additional equations to solve the problem

$$u_f = u_s \tag{4}$$

$$\theta_f = \theta_s \tag{5}$$

When pressure is applied, the hydrostatic end force has the effect of opening the joint. Therefore the bolts are stretched by an additional elongation of y_{fB} after being initially tightened to y_i. The force displacement relationship is given by

$$H_B = \frac{2(y_{fB}+y_B)K_B n_B}{\pi C} \tag{6}$$

The bolt elastic spring K_B is given by

$$K_B = \frac{E_B A_B}{\ell_B} \tag{7}$$

and the initial bolt stretch is related to the initial bolt load by

$$y_B = \frac{W\ell_B}{A_B E_B} \tag{8}$$

Using the equations of static equilibrium of force and moment in Fig. 1, the contact force H_C and its location b are expressed as

$$H_C = H_B - H_D \tag{9}$$

$$h_C = \frac{\left(H_D h_D - M_C + M + Q\dfrac{t}{2}\right)}{H_B - H_D} \tag{10}$$

Additional equations are required to determine the separation of the two flanges at any location and especially at the inner edge to facilitate the selection of the diameter of the seal. Schneider [2] applied the discontinuous beam theory to a sector of a flange that has two different widths. In order to validate this assumption for flanges with metal-to-metal contact beyond the bolt circle, it is proposed as a first step to replace the model of the discontinuous beam by a continuous or a discrete beam of a linear varying width, and as a second step, to model the flange as a circular plate with a hole in the center. Obviously, although the equations are slightly more difficult to manipulate, it allows a more precise analytical evaluation of the design parameters.

2.1 Model Based on the Discrete Beam Theory. An expression of the moment of inertia based on the varying width of an element of a unit arc of the flange (Fig. 2) and corrected for the plate effect can be written as

$$EI(x) = \frac{Et^3}{12(1-\nu^2)}\left[\frac{1-a_0}{L}x + a_0\right] \tag{11}$$

with

$$a_0 = 1 + \frac{2L}{B} \quad \text{and} \quad L = h_D + h_C \tag{12}$$

Equation (11) may be expressed as

$$EI(x) = C_{t1}x + C_{t2} \tag{13}$$

with

$$C_{t1} = \frac{Et^3}{121-\nu^2}\left[\frac{1-a_0}{L}\right] \quad \text{and} \quad C_{t2} = \frac{Et^3}{121-\nu^2}a_0 \tag{14}$$

Neglecting the edge moment M_C at the contact point where the rotation is zero, as in Ref. [2], the moment as a function of the distance x, $M(x)$ is given by

For $0 \leq x \leq h_C$

$$M(x) = \frac{H_D h_D + M + Q\ \dfrac{t}{2}}{h_C}x = C_{t3}x \tag{15}$$

with

$$C_{t3} = \frac{H_D h_D + M + Q\dfrac{t}{2}}{h_C} \tag{16}$$

For $h_C \leq x \leq L$

$$M(x) = -H_D x + H_D L + M + Q\frac{t}{2} = C_{t4}x + C_{t5} \tag{17}$$

with

$$C_{t4} = -H_D \quad \text{and} \quad C_{t5} = H_D L + M + Q\frac{t}{2} \tag{18}$$

The rotation is given by integration of the moment over EI. At the inner edge or $x=L$ this gives

$$\begin{aligned}\theta_f &= \int_0^{h_C}\frac{C_{t3}x}{C_{t1}x + C_{t2}}dx + \int_{h_C}^{L}\frac{C_{t4}x + C_{t5}}{C_{t1}x + C_{t2}}dx \\ &= \frac{C_{t3}(C_{t1}h_C - C_{t2}\ln(C_{t1}h_C + C_{t2}) + C_{t2}\ln(C_{t2}))}{{C_{t1}}^2} \\ &+ \frac{C_{t4}LC_{t1} + \ln(C_{t1}L + C_{t2})C_{t5}C_{t1} - C_{t2}C_{t4}}{{C_{t1}}^2} \\ &+ \frac{-C_{t4}h_C C_{t1} - \ln(C_{t1}h_C + C_{t2})C_{t5}C_{t1} - C_{t3}C_{t4}}{{C_{t1}}^2}\end{aligned} \tag{19}$$

The flange separation or displacement is obtained by double integration of M over EI and applying the condition that the rotation is zero at the contact reaction location

$$\begin{aligned}y_{fB} &= \frac{C_{t3}}{2C_{t1}^3}[h_C^2 C_{t1}^2 - 2(C_{t1}C_{t2}h_C - C_{t2}^2)\ln(C_{t1}h_C + C_{t2})] \\ &+ \frac{C_{t3}}{2C_{t1}^3}[2C_{t1}C_{t2}h_C(1 + \ln(C_{t2})) + 2C_{t2}^2\ln(C_{t2})]\end{aligned} \tag{20}$$

A system of equations in Eqs. (1)–(6), (9), (10), (19), and (20) is then solved for the unknowns M, Q, H_B, H_C, h_C, y_{fB}, u_f, θ_f, u_s, and θ_s.

2.2 Model Based on the Plate Theory. Young [18] expressed the deformation $y_f(r)$ and rotation $\theta_f(r)$ of a circular plate with a central hole under different boundary conditions and subjected to different loads (Fig. 3). For a circular plate clamped at the outer edge and subjected to a ring load W applied at a radius r_o

$$y_f(r) = y_{fi} + \theta_{fi}rF_1 + M_{ri}\frac{r^2}{D_f}F_2 + Q_{fi}\frac{r^3}{D_f}F_3 - W\frac{r^3}{D_f}G_3$$

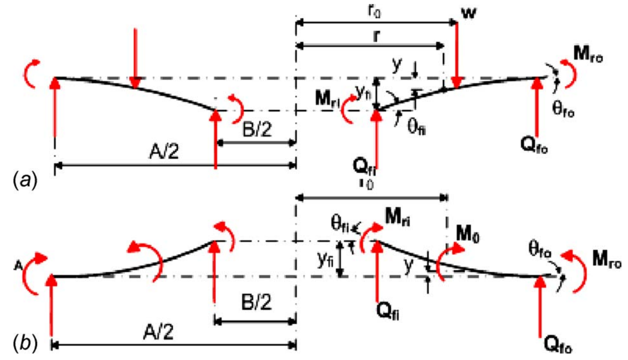

Fig. 3 Clamped circular plate subjected to (*a*) ring load and (*b*) bending moment at r_o

$$\theta_f(r) = \theta_{fi}F_4 + M_{ri}\frac{r}{D_f}F_5 + Q_{fi}\frac{r^2}{D_f}F_6 - W\frac{r^2}{D_f}G_6 \tag{21}$$

For a circular plate clamped at the outer edge and subjected to an edge moment M_o applied at a radius r_o

$$y_f(r) = y_{fi} + \theta_{fi}rF_1 + M_{ri}\frac{r^2}{D_f}F_2 + Q_{fi}\frac{r^3}{D_f}F_3 + M_0\frac{r^2}{D_f}G_2$$

$$\theta_f(r) = \theta_{fi}F_4 + M_{ri}\frac{r}{D_f}F_5 + Q_{fi}\frac{r^2}{D_f}F_6 + M_0\frac{r}{D_f}G_5 \tag{22}$$

Constants F and G are given in Ref. [18]. By application of the above to the flange case, where the contact is at some distance from the edge, the determination of flange separation due to internal pressure P is obtained.

The bolt additional stretch due to flange axial displacement and rotation at the bolt circle are obtained by superposition of the loads H_D and H_B, as given in Tables 1 and 2 for the clamped and simply supported cases, respectively. The edge loads M and Q (not shown) are such that

$$2y_{fB} = 2(y_{fB;H_D} + y_{fB;MQ} - y_{fB;H_B} - y_{fBL;H_B})$$

$$\theta_{fi} = \theta_{f;H_D} + \theta_{f;MQ} - \theta_{f;H_B} \tag{23}$$

A system of Eqs. (1)–(6), (9)–(11), (23), and (24) is then solved for the unknowns M, Q, H_B, H_C, M_C, h_C, y_{fB}, u_f, u_f, u_s, and θ_s. In the case of dissimilar flanges their respective displacement and rotation are different. Equation (23) becomes

$$\begin{aligned}y_{fB} &= y'_{fB;H_D} + y'_{fB;MQ} - y'_{fB;H_B} + \Delta y'_{fB;WH_B} + y''_{fB;H_D} + y''_{fB;MQ} - y''_{fB;H_B} \\ &+ \Delta y''_{fB;WH_B}\end{aligned} \tag{24}$$

$$\theta'_{fB} = \theta'_{BH_D} + \theta'_{BMQ} - \theta'_{BH_B}$$

$$\theta''_{fB} = \theta''_{BH_D} + \theta''_{BMQ} - \theta''_{BH_B} \tag{25}$$

Δy_{fB} is the local compression variation in the flange that can be obtained from Ref. [19]. The plate outside diameter considered for the case of a clamped edge is limited to the diameter of the location of the contact force H_C, i.e., $B+2(h_D+h_C)$. For the case where the contact force acts on the outside flange edge A, the flange is simply supported, and the equations for displacement and rotation are given in Table 2. It is to be noted that the rotation of the flange at the support edge is not equal to zero, as shown in Table 2. In this situation, one can choose as an indicator of convergence, the final bolt load H_B.

Finally, the flange separation at the gasket position can be obtained using the plate bending equations. In particular, the separation at the gasket location can indicate the suitability of the gasket knowing its resilience from the load compression test.

Table 1 Superposition of loads (clamped circular plate with a central hole)

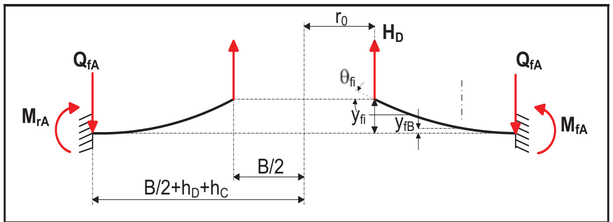

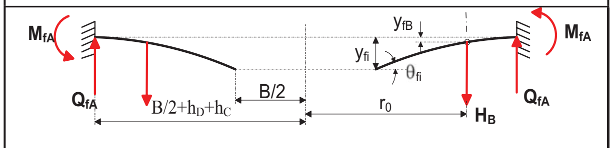

With the edge load w=H_D or H_B

$$y_{fi}=\frac{-W\ A/2^{\ 3}}{D_f}\left(\frac{C_1L_6}{C_4}-L_3\right);\ \theta_{fi}=\frac{W\ A/2^{\ 2}}{D_fC_4}L_6;$$

$$M_{fA}=-W\left(\frac{A}{2}\right)\left(L_9-\frac{C_7L_6}{C_4}\right);\ Q_{fA}=-W\frac{r_0}{A/2};$$

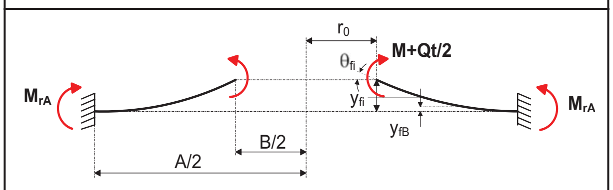

With the edge moment $M_0=M+Q\frac{t}{2}$

constants Ls and Cs are given in [3]

$$y_{fi}=\frac{M_0\ A/2^{\ 2}}{D_f}\left(\frac{C_1L_5}{C_4}-L_2\right);\quad \theta_{fi}=\frac{-M_0\ A/2}{D_fC_4}L_5;$$

$$M_{rA}=M_0\left(L_8-\frac{C_7L_5}{C_4}\right);$$

Table 2 Superposition of loads (simply supported circular plate with a central hole)

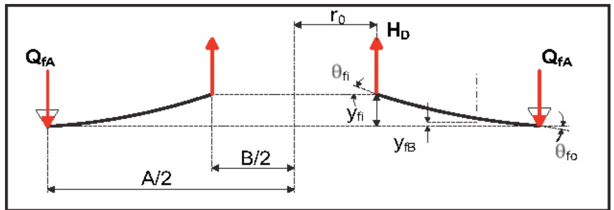

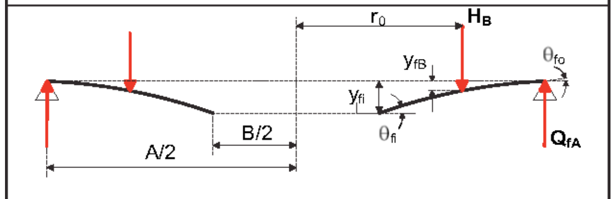

With the edge load w=H_D or H_B

$$Q_{fA}=-W\frac{r_0}{A/2};\ y_{fi}=\frac{-W\ A/2^{\ 3}}{D_f}\left(\frac{C_1L_9}{C_7}-L_3\right)$$

$$\theta_{fi}=\frac{W\ A/2^{\ 2}}{D_fC_7}L_9\ \text{and}\ \theta_{fo}=\frac{W\ A/2^{\ 2}}{D_f}\left(\frac{C_4L_9}{C_7}-L_6\right);$$

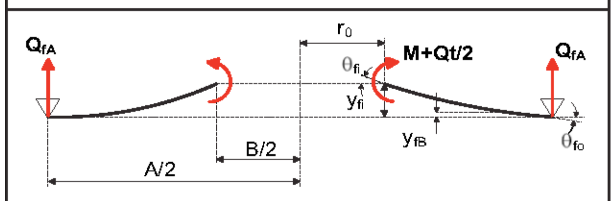

With the edge moment $M_0=M+Q\frac{t}{2}$

constants Ls and Cs are given in [3]

$$y_{fi}=\frac{M_0\ A/2^{\ 2}}{D_f}\left(\frac{C_1L_8}{C_7}-L_2\right);$$

$$\theta_{fi}=\frac{-M_0\ A/2}{D_fC_7}L_8\ \text{and}\ \theta_{fo}=\frac{-M_0\ A/2}{D_f}\left(\frac{C_4L_8}{C_7}-L_5\right);$$

3 Finite Element Model Used for Validation

ANSYS 3D 20-node solid elements SOLID169 with three degrees of freedom per node [20] were used to model the flange and bolts, as shown in Fig. 4. Because of symmetry of the geometry and loading, only one portion of the flange, delimited by the plane between two bolts and the plane passing through the bolt axis including half of the bolt, was modeled. The axial displacement of the whole flange face contact area was constrained to move down. The initial seating or bolt-up load was applied by imposing an equivalent axial displacement to all bolt nodes that belong to the section lying on the symmetrical plane.

In studying the contact between two bodies, the surface of one body is taken conventionally as a contact surface and the surface of the other body as a target surface. For rigid-flexible contact, the contact surface is associated with the deformable body, and the target surface must be the rigid surface. For flexible-flexible contact, both contact and target surfaces are associated with deformable bodies. The contact and target surfaces constitute a “contact pair.” The CONTA174 contact element is associated with the 3D target segment elements (TARGE170) using a shared real constant set number. CONTA174 is an eight-node element that is intended for general rigid-flexible and flexible-flexible contact analyses. CONTA174 is applicable to 3D geometries and is applied for contact between solid bodies or shells.

Comparisons between the two developed analytical models, i.e., the Schneider model and Finite Element Model (FEM) results, were conducted on two flange geometries of 10-in. (250 mm) and 24-in. (600 mm) inside diameter. These are carbon steel integral hubless flanges with dimensions shown in Table 3. A displacement equivalent to 24.7 ksi bolt-up stress was applied to the 10-in. flange before applying an internal pressure (100–1500

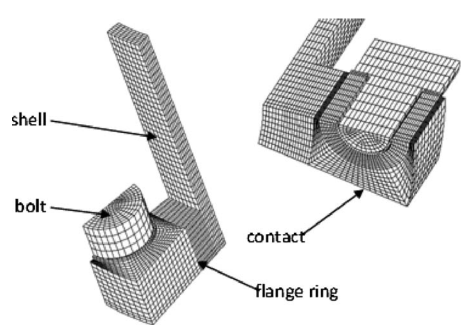

Fig. 4 3D finite element model

Table 3 Flange dimensions in inches

B	A	C	t	g_0	g_1	d_B	n_B
10	16	14	1.25	3/8	3/8	1(1/8)	16
24	32	29.5	2	1(1/16)	1(1/16)	1(1/4)	24

psi). In the case of the 24-in. flange, a 23 ksi bolt-up stress was applied before applying the internal pressure (50–450 psi). These flanges were used in pairs.

4 Comparison and Discussion of the Results

The parameters for the analysis are the contact force between the flanges, its position relative to the bolt circle, the rotation of each flange, flange separation, and the bolt stress. These parameters are important design indicators that can describe the behavior of the assembly. They are also used to compare the different methods.

Figures 5 and 6 show the contact forces and their locations as a function of pressure for both cases. These two parameters affect the calculation of moments and flange rotation. It is to be noted that for the two flanges the contact force is located between the outer edge and the bolt circle. Therefore, the rotation at the outer edge is zero and the clamped plate case is applicable. The rotation at the bore is shown in Fig. 7 for all three methods. Although the rotations are the same for the cases treated, the analytical model developed can handle assemblies of nonidentical flanges, having different rigidities (thicknesses and materials) for which the rotations will be different. It is worth noting that if the internal pressure of the fluid increases, the contact between the flanges move to the outer edge of flange and separation will be higher. In the case where the fluid pressure is relatively large, the contact is at the outer edge, and the flange rotation at this location is not null. Table 4 shows the comparison of the bore rotation of the two flanges with FEM for internal pressures of 200 psi and 400 psi applied to flanges of 10-in. and 24-in., respectively. Even though the rotations are slightly higher with FEM due to the presence of the holes, the beam and plate theories give good predictions.

On the sealing point of view, separation between the two flanges is the main parameter to determine if the compression on the seal in the operating conditions is adequate. Figure 8 shows flange separation at the bore as a function of pressure for the models compared with FEM and summarized in Table 5. The values obtained by the numerical finite element models are a benchmark to evaluate the analytical models. The models based on plate and continuous beam theories compare well with finite element analysis relative to the continuous beam model. In addition, at the higher pressures, the discontinuous beam model predicts much lower separation than the other two models. This in-

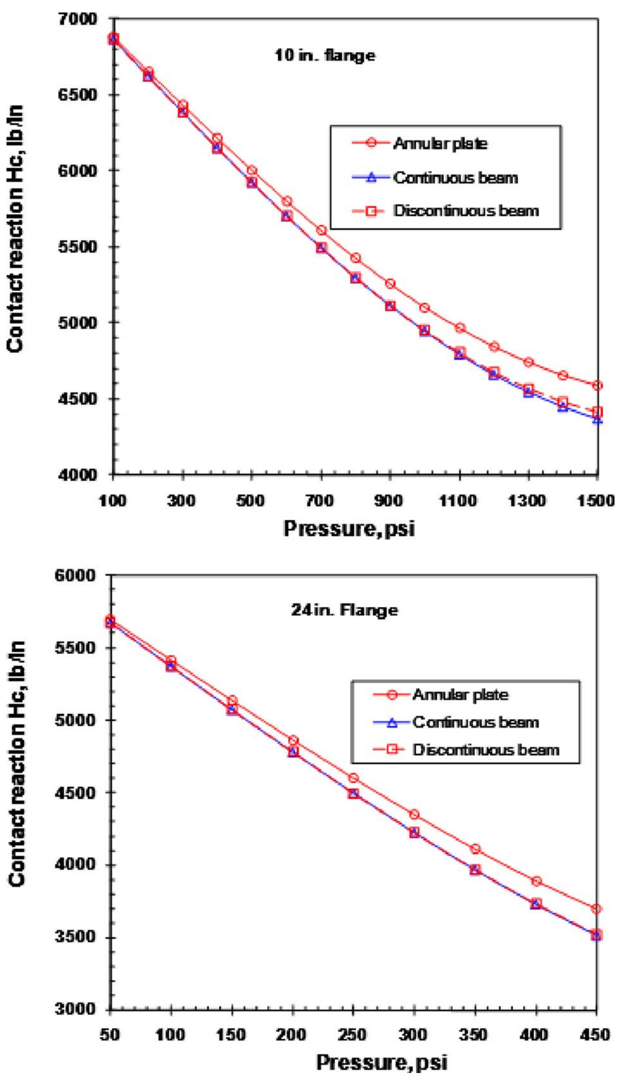

Fig. 5 Contact force variation with pressure

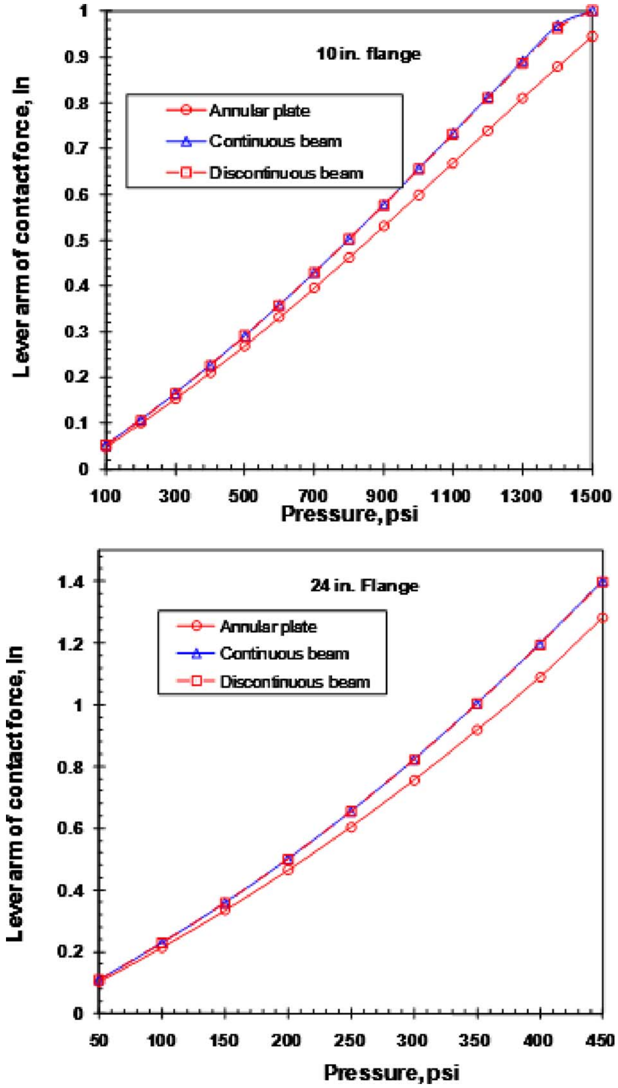

Fig. 6 Variation in the contact force position with pressure

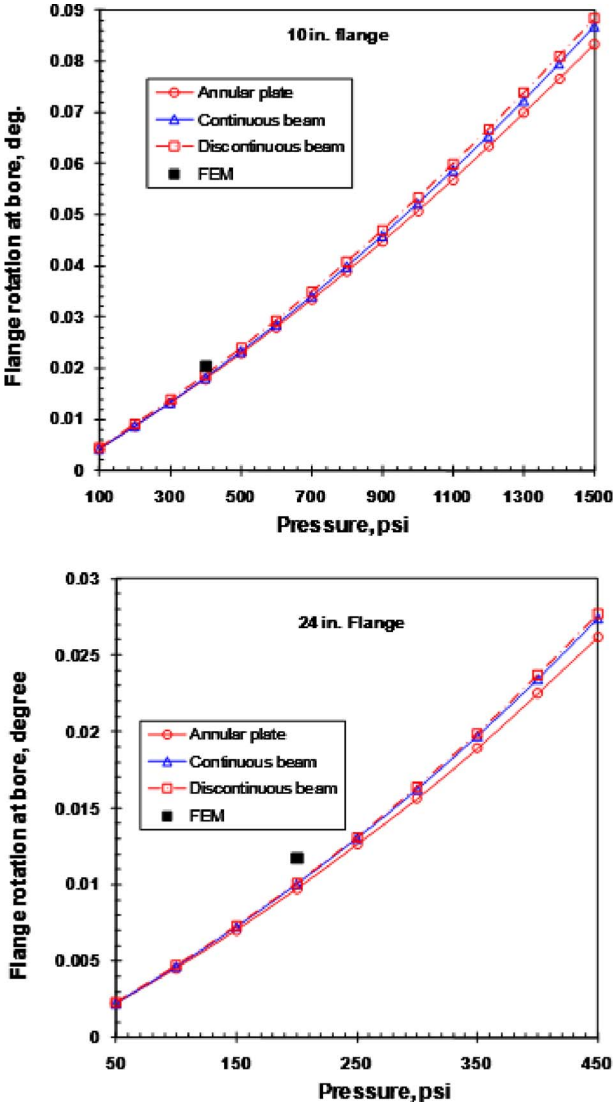

Fig. 7 Rotation variation at the flange ID with pressure

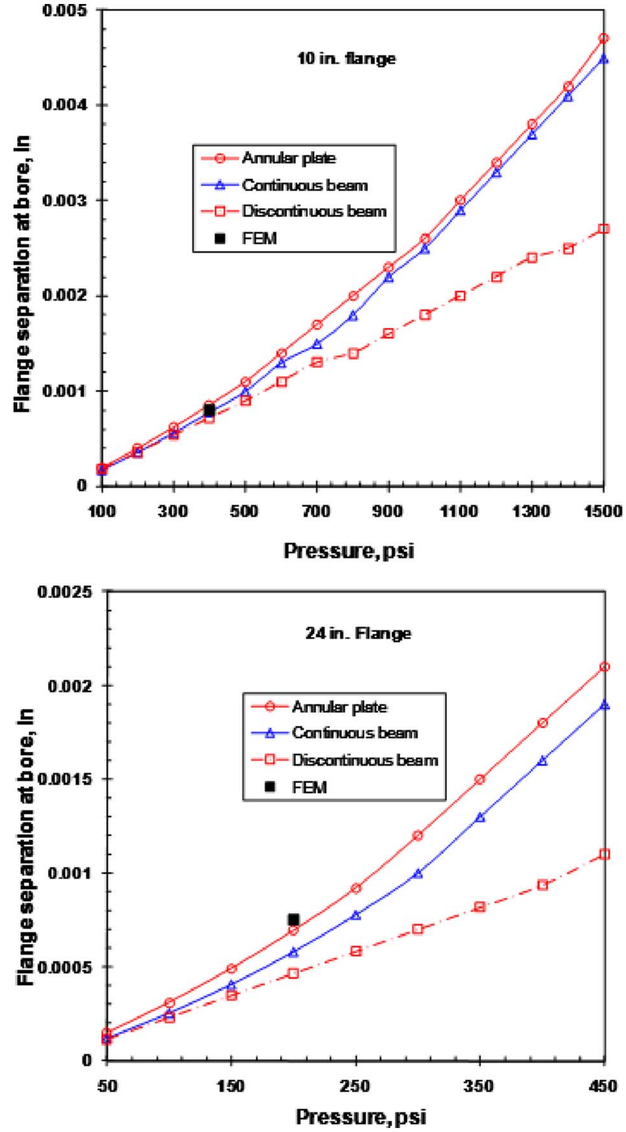

Fig. 8 Comparison of the flange separation at the bore with the three models

dicates that there will be cases where the modeling of circular flanges by beam theory may not be conservative.

Figures 9 and 10 show the radial distribution of the flange contact stress and separation obtained from the FE study. The separation from the plate model is added for comparison. A liftoff is shown at the bore vicinity during boltup and slightly bigger during operation. The metal-to-metal contact flanges have the advantage of not bending the flanges comparatively to raised face flanges. The contact pressure between the two flanges is much higher at the bolt position than between bolts. Nevertheless, the separation at these two locations is very similar and very close to that predicted by the analytical model based on the plate theory. This suggests that the variation of separation in the circumferential direction is not significant. Obviously, in general, separation is not constant and depends on bolt spacing. Notwithstanding, such information is useful to select the position of the seal based on its ability to spring back. The elastic recovery of the gasket is necessary to fill the space produced by flange separation as a result of the pressure and other external loads. Furthermore, in order to maintain a sufficient force on the seal, it is recommended to locate the latter as close as possible to the bolt hole, where flange separation is relatively smaller compared with that at the bore. However, as a trade off, this may result in a higher hydrostatic end force.

Another parameter worth investigating is the bolt load variation with pressure. It is clear that the bolt load always increases since

Table 4 Flange rotation

	Flange rotation at bore (deg)			
Flange	Schneider	Continuous beam theory	Plate theory	FEM
B10	0.0187	0.0182	0.0179	0.0204
B24	0.0101	0.0100	0.0097	0.0117

Table 5 Flange separation comparison with FEM

	Separation at the bore (mils)			
Flange (pressure)	Schneider	Continuous beam theory	Plate theory	FEM
B10 (400 psi)	0.72	0.78	0.84	0.8
B24 (200 psi)	0.47	0.58	0.69	0.75

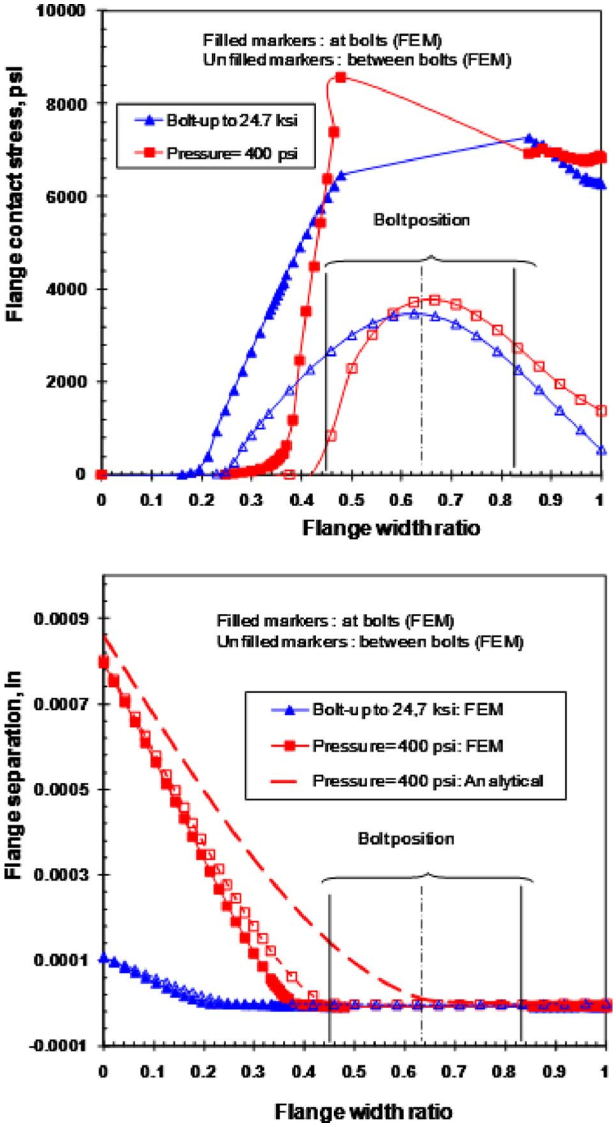

Fig. 9 Contact stress and separation in 10-in. flange

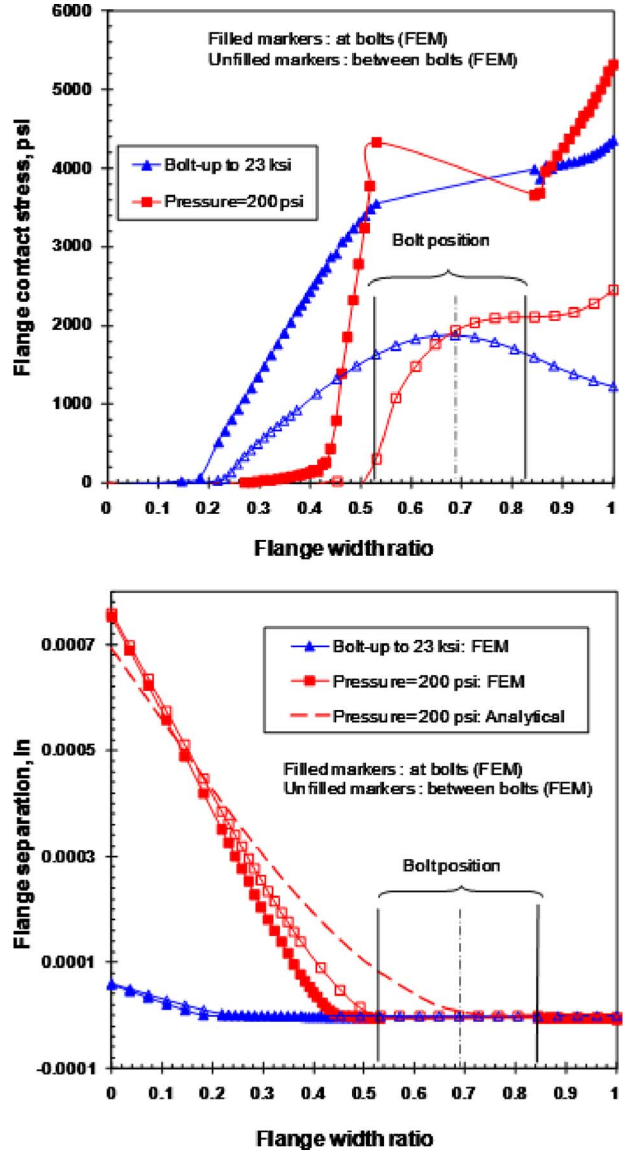

Fig. 10 Contact stress and separation in 24-in. flange

separation causes the bolt to elongate more. It is therefore important to evaluate the amount of increase especially if the bolts are tightened near yield or subject to fatigue. Figure 11 shows the comparison between the three models as the pressure is increased in the two cases. While the increase is somewhat exponential, it remains that there is a good agreement between the three methods. In addition, Table 6 includes the FEM results for validation.

5 Conclusion

An analytical method has been developed to analyze flanged joints with metal-to-metal contact beyond the bolt circle. This method provides additional considerations comparatively to the current method when designing such flanges. The developed model based on the plate theory has the advantage of showing rationality and consistency in the approach of treating metal-to-metal flanges since the same structural theoretical analysis as raised face flanges is used. Besides being more comprehensive, the model based on the plate theory gives more confidence on its ability to predict flange separation and the bolt load increase during operation.

Nomenclature

β = $[6(1-\nu^2)/Bg_0]^{1/4}$
θ = rotation (rad)
ν = flange Poisson ratio
γ = $\nu+(K^2+1)/(K^2-1)$
A = flange outside diameter (in.)
A_B = total bolt stress area (in.^{2})
A_p = pressurized area encircled by flange ID (in.^{2})
B = flange inside diameter (in.)
C = bolt circle diameter (in.)
d_B = bolt nominal diameter (in.)
D_0 = flange centroid diameter (in.)
E = modulus of elasticity (psi)
g_0 = shell thickness (in.)
g_1 = hub thickness (in.)
H_B = bolt force (lb)
H_C = contact force (lb)
H_D = hydrostatic end force (lb)
h_C = radial distance from the bolt circle to H_C (in.)
h_D = radial distance from the bolt circle to H_D (in.)
K = ratio of outside diameter to inside diameter of flange (A/B)
K_B = bolt uniaxial stiffness (lb/in.)

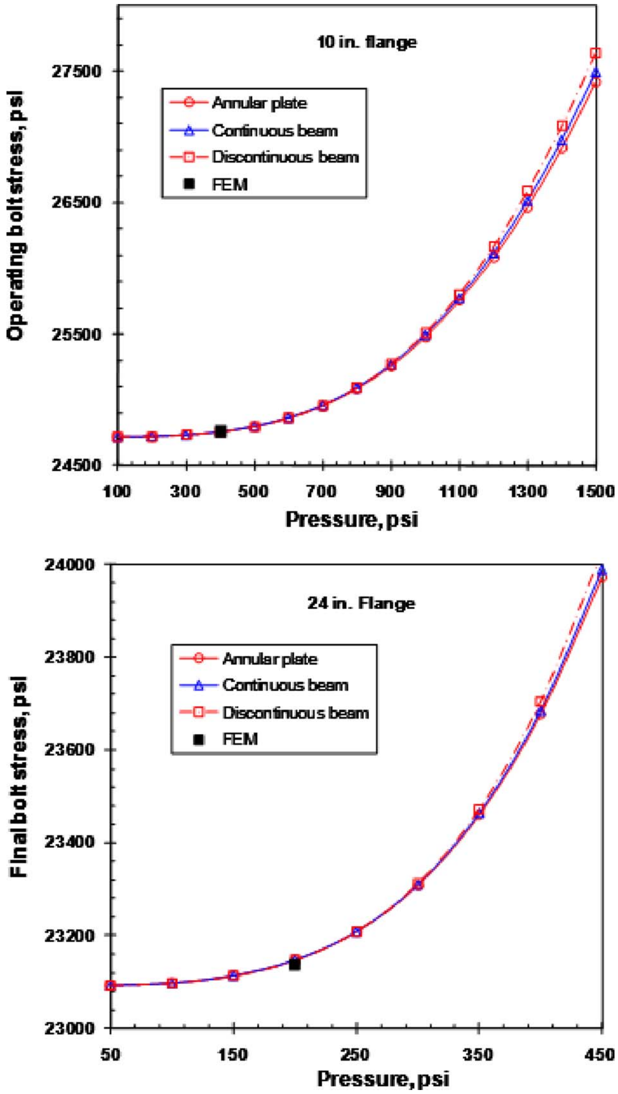

Fig. 11 Bolt load increase with pressure

ℓ_B = initial effective bolt length (in.)
L = equal to H_C+H_D (in.)
M = discontinuity edge moment (in.lb/in.)
M_C = moment per unit circumference at the flange contact (in.lb/in.)

Table 6 Bolt load increase

Flange		Bolt stress (psi) Schneider	Continuous beam theory	Plate theory	FEM
B10	Boltup	24,715	24,715	24,715	24,715
	Pressure	24,754	24,756	24,754	24,761
B24	Boltup	23,092	23,092	23,092	23,092
	Pressure	23,147	23,148	23,147	23,137

M_f = flange moment per unit circumference (in.lb/in.)
n_B = number of bolts
P = pressure (psi)
Q = discontinuity edge load (lb/in.)
t = flange thickness (in.)
u = radial displacement (in.)
W = initial bolt load (lb)
Y = axial defection (in.)

Subscript

B = refers to the bolt
f = refers to the flange
P = refers to the pressure
M = refers to the moment
S = refers to shell

Superscript

i = refers to the initial bolt-up condition
f = refers to the final operating condition

References

[1] Webjörn, J., 1967, "Flange Design in Sweden," ASME Paper No. 67-PET-20.
[2] Schneider, R. W., 1968, "Flat Faces Flanges With Metal-to-Metal Contact Beyond the Bolt Circle," ASME J. Eng. Power, **90**(1), pp. 82–88.
[3] 2007 "Flat Face Flanges With Metal-to-Metal Contact Outside the Bolt Circle," ASME Boiler and Pressure Vessel Code, Sec. VIII, Div. 1, Appendix Y.
[4] Pindera, J. T., and Sze, Y., 1972, "Influence of the Bolt System on the Response of the Face-to-Face Flanged Connections," Proceedings of the Second International Conference on Structural Mechanics in Reactor Technology, Vol. G, Paper No. 2/6.
[5] Webjörn, J., and Schneider, R. W., 1980, "Functional Test of a Vessel With Compact Flanges in Metal-to-Metal Contact," Weld. Res. Counc. Bull., **262**, pp. 10–16.
[6] Webjörn, J., 1985, "New Look at Bolted Joint Design," Mach. Des., **57**(14), pp. 81–84.
[7] Webjörn, J., 1985, "The Bolted Joint—A Series of Problems," dissertation No. 130, Department of Science and Technology, Linköping University, Linköping Sweden.
[8] Webjörn, J., 1989, "An Alternative Bolted Joint for Pipe-Work," Proc. Inst. Mech. Eng., Part E, **203**, pp. 135–138.
[9] Lewis, L. V., Fessler, H., and Hyde, T. H., 1987, "Determination of Initial Gaps Between Flat Flanges Without Gaskets," Proc. Inst. Mech. Eng., Part A, **201**, pp. 267–277.
[10] Fessler, H., Hyde, T. H., and Lewis, L. V., 1988, "Leakage Through Loaded Flat-Flanged Joints Without Gaskets," Proc. Inst. Mech. Eng., Part A, **202**, pp. 1–13.
[11] Hyde, T. H., Lewis, L. V., and Fessler, H., 1988, "Bolting and Loss of Contact Between Cylindrical Flat Flanged Joints Without Gaskets," J. Strain Anal. Eng. Des., **23**, pp. 1–8.
[12] Hyde, T. H., Fessler, H., and Lewis, L. V., 1994, "The Sealing of Conical Faced Flanges Without Gaskets," Proceedings of the Seventh International Conference on Pressure Vessel Technology, ICPVT-7, pp. 105–118.
[13] Abid, M., and Nash, D. H., 2003, "Comparative Study of the Behaviour of Conventional Gasketed and Compact Non-Gasketed Flanged Pipe Joints Under Bolt-Up and Operating Conditions," Int. J. Pressure Vessels Piping, **80**(12), pp. 831–841.
[14] Joshi, D., Mahadevan, P., Marathe, A., and Chatterjee, A., 2007, "Unimportance of Geometric Nonlinearity in Analysis of Flanged Joints With Metal-to-Metal Contact," Int. J. Pressure Vessels Piping, **84**(7), pp. 405–411.
[15] Power, D. J., and Nash, D. H., 1999, "Comparison of the Sealing Contact Behaviour of Standard and Compact Metal-to-Metal Bolted Flanges," ASME Pressure Vessels and Piping Division, PVP-Vol. 382, pp. 79–86.
[16] Abid, M., and Nash, D. H., 2004, "A Parametric Study of Metal-to-Metal Contact Flanges With Optimised Geometry for Safe Stress and No-Leak Conditions," Int. J. Pressure Vessels Piping, **81**(1), pp. 67–74.
[17] Timoshenko, S., 1927, "Flat Ring and Hubbed Flanges," Mech. Eng. (Am. Soc. Mech. Eng.), **49**, pp. 1343–1345.
[18] Young, W. C., 2002, *Roark's Formulas for Stress and Strain*, 7th ed., McGraw-Hill, New York.
[19] Shigley, J. E., and Mischke, C. R., 1989, *Mechanical Engineering Design*, 5th ed., McGraw-Hill, New York.
[20] ANSYS, 2006, ANSYS Standard Manual, Version 11.0.